

# Nanoscale

Accepted Manuscript



This is an *Accepted Manuscript*, which has been through the Royal Society of Chemistry peer review process and has been accepted for publication.

*Accepted Manuscripts* are published online shortly after acceptance, before technical editing, formatting and proof reading. Using this free service, authors can make their results available to the community, in citable form, before we publish the edited article. We will replace this *Accepted Manuscript* with the edited and formatted *Advance Article* as soon as it is available.

You can find more information about *Accepted Manuscripts* in the [Information for Authors](#).

Please note that technical editing may introduce minor changes to the text and/or graphics, which may alter content. The journal's standard [Terms & Conditions](#) and the [Ethical guidelines](#) still apply. In no event shall the Royal Society of Chemistry be held responsible for any errors or omissions in this *Accepted Manuscript* or any consequences arising from the use of any information it contains.

# Helical Metallic Micro- and Nano-structures: Fabrication and Application

Lichun Liu<sup>a</sup>, Liqiu Zhang<sup>a</sup>, Sangmin Kim<sup>b</sup>, and Sungho Park<sup>b,\*</sup>

<sup>a</sup>College of Biological, Chemical Sciences and Engineering, Jiaying University, 314-001, China.

<sup>b</sup>Department of Chemistry, BK21 School of Chemical Materials Science, and Department of Energy Science, Sungkyunkwan University, Suwon 440-746, South Korea.

E-mail: [spark72@skku.edu](mailto:spark72@skku.edu) (S. Park)

## Abstract:

Metal elements occupy more than 70% of the positions in the periodic table, and their use has accelerated human civilization due to their invaluable chemical and physical characteristics. With the rapid development of metals, various structures of microscopic metal particles have been fabricated and investigated as functional materials in scientific research and practical applications. The phrase ‘structure determines properties’ has been widely acknowledged as a golden rule in chemistry and materials science, especially when the size of small particles is in the micro- or nanoscale dimension. Helical metallic micro- and nano-structures with complex shapes have recently emerged and may be used for various useful applications such as photonics, sensors, actuators, micro-/nano-robotics, micro-/nano-electronics, based on their unique mechanical, electrical, and electromagnetic properties. This review paper specifically concerns the fabrication and application of helical metal structures with a feature size ranging from micro- to nano-sized. The unusual spatial distribution of active atoms in helical metallic micro- and nano-structures and their helical morphology could offer new opportunities for applications beyond those of other conventional metal and nonmetal micro- and nano-structures.

## 1 Introduction

The phrase ‘structure determines properties’ is a well-known rule in science, especially for small metallic materials with micro- and nano-scale dimensions principally due to the greater exposure of surface atoms.<sup>1-3</sup> The atoms with free outermost shell electrons in a micro- and nano-scale inorganic metal material are fundamentally critical to most practical applications; therefore, how metal atoms form a micro- or nano-structure strongly influence the properties of a metallic material. Metallic micro- and nano-structures with shapes resembling spheres, cubes, prisms, and disks have been extensively reported with detailed scientific insights in recent decades, and enhanced performance was observed in most relevant applications such as photonics, sensors, and catalysis.<sup>4,5</sup> In addition to these metallic micro- and nano-structure shapes, a more fascinating and complex shape, the helix, has drawn considerable attention from academic circles. A helix is one of the most fundamental geometrical structures in nature. This helical shape of materials exhibits distinctive mechanical, chemical, and physical properties. One of the most popular examples of a metallic helical shape is a compressible spring that is commonly observed in machinery and plays a significant mechanical role. The basic parameters of a typical helical coil are shown in Fig. 1.

Due to the soft nature of organic materials, a number of articles reported the successful synthesis of helical organic, polymeric, and even semiconducting materials primarily based on molecular self-assembly.<sup>6-9</sup> Helical metallic structures with micro- and nanoscale dimension are scarcely fabricated via self-assembly as used for helical ones of organic materials. Since metals have played a fundamental role in human history, helical metallic structures are also of potential importance in many fields, just as compressible metal springs are used widely in the macroscale world. Most devices are progressing towards miniaturization for low-cost production and easy portability. Helical metallic micro- and nano-structures as functional components have considerable promise for future miniaturized devices. To specifically spotlight the

newly emerged material, this review paper investigates the fabrication and application of helical metallic structures with micro- and nano-scale dimensions.

## 2 Fabrication

The fabrication of materials is the cornerstone of research and applications. Because helical metallic micro- and nano-structures are rather complex and microscopic, the interactive forces between metal atoms are strong and their fabrication challenging. Most fabrication methods of helical micro- and nano-structures are dependent on bottom-up methodologies via controlled growth. Fewer fabrications employed top-down strategies through etching and curling processes. To date, the fabrication strategies of helical metallic micro- and nano-structures primarily consist of oblique angle-based deposition, templates, and coatings.

### Oblique angle-based deposition

A useful technique with good controllability and reproducibility for the fabrication of three-dimensional columnar micro- and nano-structures on a substrate is oblique angle deposition (OAD)<sup>10</sup>, which utilizes an oblique incident physical vapor flux to deposit target materials on a substrate. As the vapor atoms condense and nucleate on the substrate, the shadowed regions behind each nucleating grain cannot receive incoming vapor atoms with the site-competitive growth of grains, resulting in a porous film with isolated columns of material (Fig. 2). Originating from this technique, glancing angle deposition (GLAD) was developed by rotating the substrate in both polar and azimuthal directions during the OAD process. This technique is a powerful method of forming a helical structure because only the substrate rotation is introduced in the OAD technique. GLAD has been successfully utilized to synthesize many nano-structures such as spirals, pillars, zigzags, and branched columns on a substrate film.<sup>11</sup>

In 1996, Robbie et al. reported the fabrication of Cr, Mg, Cu, and MgF<sub>2</sub>, SiO, CaF<sub>2</sub> helical nano-structures with pitches ranging from 50 to 2000 nm on a glass substrate using the GLAD technique.<sup>12</sup> The fine controllability on three-dimensional helical column on a film allows the dimensional tailoring of less than 10 nm. As-synthesized nano-structures are chiral and can potentially create optical activity due to the rotation of the plane of light polarization. Measurements of the optical rotatory dispersion of the helical structure film revealed their optical activity. As a comparison, no optical rotation was observed for a glass substrate without helical nano-structures.

Mark et al. successfully utilized the GLAD technique to synthesize nanocolloids for a wide range of materials with anisotropic three-dimensional shapes and controllable compositions, as shown in the synthetic procedure illustrated in Fig. 3.<sup>13</sup> The starting homogeneous nucleation sites were 14-nm Au nanodots patterned by micellar nanolithography. The materials were deposited by physical vapor deposition at a grazing incidence. A cooling substrate strategy was used to overcome the high surface mobile evaporants so that the high-energy shape of a material could be preserved. Several helical structures were successfully synthesized using this method, including Cu, Au, and an Ag-Cu alloy. Most of fabrication methodologies couldn't control the compositions of the metallic helices. However, this method is able to simultaneously control both compositions and shapes of helices.

Some other articles reported the successful fabrication of helical metallic micro- and nano-structures. A study by Kesapragada et al. demonstrated the successful fabrication of a Cr zigzag helical nano-structure 15–55 nm wide on the SiO<sub>2</sub>/Si substrate using the GLAD technique.<sup>14</sup> A two-turn, eight-armed, rectangular Si/Ni heterogeneous helical structure (height, ~1.98 μm) on a Si substrate was fabricated using a multilayer GLAD technique (Fig. 4).<sup>15</sup> The structures were composed of alternating layers of amorphous Si and face-centered cubic Ni. Chen et al. demonstrated the successful fabrication of a single crystal helical porous Cu (100) nanostructure using GLAD.<sup>16</sup> As shown in Fig. 5, the products prepared by OAD and GLAD differ because of the

introduction of substrate rotation in OAD. Helical Ag nanorod arrays with different numbers of arms (3–8 arms) were synthesized on a glass substrate by OAD as reported by Zhou et al.<sup>17</sup> A custom-built electron-beam evaporation system was used to deposit Ag with an incident flux angle  $86^\circ$ . A quartz crystal microbalance (QCM) was used to control the thickness of the helical Ag nanorod film. The GLAD technique is rather important in the fabrication of helical structures witnessed from abovementioned cases. It should be preferentially considered to use due to its intrinsic feature when one wants to achieve helical micro- and nano-structures. However, the shape of helices reported in the literature is not all well-shaped, such as zigzag shape. This imperfect structure probably cannot be useful as helices with a spring shape.

### **Template-oriented fabrication**

Use of a sacrificial template is an interesting fabrication methodology for helices and is one of the most fundamental methods in nanomaterial synthesis. This method is a process in which the target materials are first deposited in/on a template material and the template is subsequently removed by a chemical or physical post-treatment. The nano-structures synthesized by the template method usually inherit the shape of nanospaces in a template owing to the nano-confinement effect. However, various shapes of materials other than inherited shapes have been found in template fabrication. Thus, it indicates that the template strategy provides more flexible control of the target material growth. Some pieces of articles have conceptually demonstrated the fabrication of helical metal micro- and nano-structures based on hard and soft templates.

Kamata and coworkers reported a biotemplating method to synthesize a metal micro-helix (Fig. 6). The helical vessel exists in every part of vascular plants. The helical vessel was creatively utilized in this work as a template, on which electroless silver plating produced a silver coating on vessels while preserving the helical shape of the vessels.<sup>18</sup>

Palladium nanohelices have been synthesized using a hard template (anodic aluminum oxide, AAO), electrochemical Pd-Cu co-deposition, and selective wet-chemical etching of non-noble Cu (Fig. 7).<sup>19-21</sup> An AAO template can be easily and completely removed within minutes by a concentrated sodium hydroxide solution. In this experimental nanotechnology, large-scale nanohelices are easily produced at low cost and in short periods of time. The resulting Pd nanohelix exhibits a well-defined spring-like helical structure. The formation of the Pd nanohelix was attributed to the screw dislocation effect of crystal growth in alumina nanochannels. This hard template method shows good dimensional control due to mature AAO production technology. The length of the nanohelix was controlled by the charge amount of electrochemical deposition and the thickness of the AAO template, and the diameter was tuned by altering the nanochannel size in the AAO templates.

Wu and coworkers presented a systematic study of the confined assembly of silica-surfactant composite mesostructures within cylindrical nanochannels. The same precursors and reaction conditions that generate two-dimensional hexagonal SBA-15 were used in a template-assisted synthesis. Instead of SBA-15 silica, helical silica can form directly inside the physically-confined nanochannels of the AAO template via self-assembly. The insulating property of helical mesoporous silica can facilitate use as a secondary template to deposit target materials using electrochemical deposition. With this kind of secondary template, helical Ag and Ni nanowires have been fabricated successfully.<sup>22</sup> Gansel et al. established a method to fabricate a gold microhelix using an air helix template in a polymer film produced by 3D direct laser writing (DLW) and subsequent electrochemical gold plating (Fig. 8). The polymer template could be readily removed by plasma etching. The resulting gold helix was characterized as a photonic metamaterial and the photonic properties of the gold helix depended on the handedness and number of pitches.<sup>23</sup>

The gold nanohelix has been synthesized by nanomotor-based biocatalytic patterning (Fig. 9). An Au/Ag/Ni hybrid nanorod was used as a nanomotor whose reproducible

rotation was caused by the Ni segment responding to the external rotating magnetic field. Glucose oxidase (GOx) was first immobilized on the Au end of the hybrid nanorod. In a solution containing glucose and  $\text{AuCl}_4^-$  ions, biometallization occurred and Au was deposited due to the yield of the  $\text{H}_2\text{O}_2$  reducing agent in the glucose catalytic oxidation. The controlled rotation helped to form a helical Au microstructure.<sup>24</sup> Inoue et al. employed 1-dodecanesulfonate assemblies as a template and a homogeneous precipitation method using urea to synthesize micro-helical ruthenium compound structures with various sophisticated morphologies, porous and solid interiors. The formation of such sophisticated helical morphologies is likely controlled by cooperative assembly between surfactants and inorganic species. Helical ruthenium could be obtained by the hydrogen reduction treatment of the ruthenium compound product.<sup>25</sup> Takahashi et al. demonstrated that surfactant tubules can be used as a soft template in solution to synthesize mono-, double-, and multi-helical gold nanowires that depend heavily on experimental conditions. The formation of a helical structure in this method was primarily affected by the presence and absence of a surfactant in the electroless plating solution.<sup>26</sup>

Templating method is simple to fabricate metallic helices with micro- and nano-dimensions, but, there is only several articles reported successful fabrication of metallic helices. This method seems hard to fabricate metallic helical with a wide range of materials.

### **Rolled-up strategy**

Top-down-based, rolled-up nanotechnology can be employed to fabricate a helical metal structure by exploiting a pre-strained and crystal lattice mismatched bilayer membrane.<sup>27-31</sup> For example, a metal nanobelt 3D helix with controllable helicity angle, chirality, diameter, and pitch size could be synthesized by depositing a metal layer on the strained semiconductor SiGe/Si bilayer and subsequently rolling up the layered structure through wet-chemical etching of the bottom SiGe layer, as reported by Zhang et al (Fig. 10).<sup>32,33</sup> The spontaneous rolling of the layered structure could



form a nanobelt helix that is directed by the Young's modulus. This method is of importance in helix production due to its excellent control of the helix parameters. Additionally, Li et al. reported successful synthesis of Ti micro-helices using an analogous concept.<sup>34</sup> In the core process of this rolled-up method only involves the shape change which is a physical change differing from many other chemistry-dependent methods. Learning from present cases, we believe that more and more helical metallic helices can be fabricated by employing this method. To prepare appropriate strain and crystal lattice mismatch may be a major obstacle for general use in future.

### **Metal coating on helical structures**

Apart from directly obtaining helical metal structures using the above-mentioned routes, a general strategy to form a helical metal structure is to coat atomic metals on the surface of another well-established metal or nonmetal helical structures with micro- or nanoscale dimensions. This is a very promising strategy to achieve a wide range of helical metallic micro- and nano-structures, and the coating-induced core-shell structure will be of use in many applications because only surface metal atoms affect many applications, which is especially good for costly noble metals that impact product cost. From this viewpoint, the helical structure of all metals theoretically achievable just through developing a substrate helical material with fine-controlled dimension and developing effective coating methods for metals. This method can be also considered as templating method, in which substrate helices function as templates. In view of the importance and universality of this strategy, we specifically list it as an independent category. Coating is actually a post-treatment process after helices fabrication. Most critically, coating can be useful to produce a metal helix from a non-metal helical structure.

For example, Singh et al. have conducted a study on the fabrication of a plasmonic metal-coated structure. In this work, a dielectric helix, such as SiO<sub>2</sub> and MgF<sub>2</sub>, were

firstly synthesized using the common GLAD technique. Then, a target plasmonic Ag metal was evaporated on the as-synthesized helical structure resulting in a metal-coated helix.<sup>35</sup> This is a typical one of coating cases that possess the easy-to-make helical shape, at the same time, exhibit properties of coated materials. Except for three-dimensional helices, planar helices are also reported. A micro-electro mechanical system (MEMS) technology was used to engineer a deformable helical structure.<sup>36</sup> Prior to fabrication, the active buried Si oxide layer was highly doped with phosphate by thermal diffusion. The helical shape was then patterned via photolithography and deep reactive ion etching. After releasing the handling layer by hydrofluoric acid vapor etching, a freestanding planar helix was achieved. To obtain a metallic Au helical structure, E-beam evaporation was used to deposit the Au layer on the prepared Si helical structure. Resulted coating on a helix usually homogeneous and smooth, sometimes the coating may be different. Sai et al. utilized Si nanohelices as a substrate to coat noble metal nanoparticles, including Au, Ag and Au@Ag, using plasma-enhanced chemical vapor deposition (PECVD) and chemisorption strategies, resulting in a large surface-to-volume ratio of SERS active media.<sup>37</sup> Lilly et al. made use of CdTe nanoparticle assembled twisted nanoribbon as a building block to grow Au nanoparticles via a chemical reaction, giving rise to a helical Au structure.<sup>38</sup>

Singh et al. made an attempt to synthesize the four-turn Si nanohelices using a GLAD technique, and then coated a 10-nm-thick Co layer on the nanohelices using chemical vapor deposition.<sup>39</sup> Tottori et al. prepared a microscale helical polymer structure by a direct laser-writing technique using negative-tone photoresist strategies. The Ni/Ti thin bilayers were then deposited on the helical polymer structure by e-beam evaporation to obtain metal-coated micro-helices.<sup>40</sup> Zhan et al. fabricated helical organogel ribbons using a racemic gelator and the subsequent reduction of silver cations adsorbed on the helical ribbons with sodium borohydride yielded right-, left-handed and double-stranded Ag-coated helical nano-structures.<sup>41</sup> Inspired by nature, the helical form of artificial bacterial flagella (ABF) was designed and successfully fabricated by Qiu et al. Subsequent Fe-coating (for magnetic actuation)

on the ABFs using electron beam deposition could contribute little cytotoxicity and have potential for *in vivo* applications.<sup>42</sup>

In order to obtain helical structure with a specific metal on the surface, a desired metal is even coated on a helical structure of another metal. On the basis of Pd nanosprings fabricated using template assisted electrodeposition<sup>19</sup>, Wang et al. implemented the fabrication of helical nanoswimmers with controlled pitches and diameters by Ni coating.<sup>21</sup> This case exactly shows the usefulness of coating on the fabrication of helical metallic micro- and nano-structures. Using this method, on the premise of a well-developed helix fabrication method, the fabrication difficulty is shunted to coating process.

#### **Other fabrication methods**

There are still some other minor methods developed for fabrication of helical metallic micro- and nano-structures. Chang et al. developed a modified electrospinning method for the fabrication of micro-sized copper oxide and iron oxide nanohelices. A fiber bundle used as an axis was fabricated by electrospinning. Another electrospinning process using a stream of copper nitrate within a PVP sol was also performed to wind around the prepared bundle. The electrospun material was copper oxide. To obtain a metallic copper nanohelix, they exploited hydrogen post-treatment to convert copper oxide to copper.<sup>43</sup>

Self-assembly is one of most important methods for synthesizing helical metallic structures which often involves the assistance from the organic or biological molecules.<sup>44-46</sup> Left-handed gold nanoparticle double helices were synthesized by controlling the moiety of amino acids in the peptide chain (Fig. 11).<sup>47-49</sup> The methodology consists of two simultaneous processes, including peptide self-assembly and peptide-based nucleation of discrete nanoparticles. As in many inorganic nanoparticle syntheses, the organic molecules are typically used to assist the growth of the components. In these works, researchers were able to control the formation of

gold nanoparticle superstructures by adjusting the peptide composition at the molecular level. In another article reported by Sharma et al., Au nanoparticle-assembled helical structures were formed by DNA mediation. By attaching single-stranded DNA to gold nanoparticles, helical nanotube structures ranging from stacked rings to single, double, and nested helices have been self-assembled.<sup>50</sup>

### 3 Applications

The final goal of any materials research is to apply novel materials to real life. Helical metallic micro- and nano-structures have several applications including as sensors, inductors, nanoelectronics, optical polarizers, and catalysts. The special shape of helical metallic micro- and nano-structures leads to distinctive applications. The metallic compositions allow for various applications like other metal micro- and nanoparticles have been extensively applied. First of all, the helical metallic micro- and nano-structures bearing spring shape may function as microscopic compressible springs as used in the machines. Currently, direct use of so tiny helices as compressible springs in micro- and nano-machines is impossible, because such machines are still too hard to manufacture. However, elasticity of some helices endows them with use as microscopic force or pressure sensors. In addition, colloidal or arrayed metallic helices possess small sizes that comparable to the wavelength of ultraviolet, visible and infrared light waves. This feature of the metallic helices guarantees their application in photonics. Another more important application should be in locomotion which is usually assisted by an external magnetic field.

#### Photonics

Light is a kind of electromagnetic radiation that consists of an electric and magnetic field that oscillate perpendicular to one another and also to the propagating direction. Light properties change when light transmits through a surface composed of ordered micro- or nano-structures with special shapes. Helical and optically active

nano-structures can be divided into categories of left-handed and right-handed chirality depending on the clockwise and counter-clockwise turning of the structures. Mark et al. combined low-temperature shadow deposition with nanoscale patterning to synthesize a variety of nanocolloids (magnetic, plasmonic, dielectric, semi-conducting and alloyed materials) with anisotropic three-dimensional helical shapes down to a 20-nm feature size.<sup>13</sup> Circular dichroism (CD), the differential absorption of left and right circularly polarized light, was used to characterize the property change of light. This technique has a high resolution and versatility in synthesizing complex 3D nano-structures that show tunable chiroptical response in the visible region by CD spectroscopy as shown in the example in Fig. 12. The chiroptical properties of helical structures were also demonstrated in other articles.<sup>35,36,47</sup>

Gansel et al. reported that a microscale gold helix could be applied as a photonic metamaterial for a broadband circular polarizer.<sup>23</sup> Figure 13 shows experimental and theoretical transmittance spectroscopy in the wavelength range of 3–8.5  $\mu\text{m}$  using left- and right-handed helical Au structures with different turns.

### Sensors

Owing to the flexible shape and metal-dominant compositions, helical metallic micro- and nano-structures are naturally useful as force (or pressure) sensors resembling conventional compressible springs that are used as parts of machines and devices.

The mechanical properties of the helical metallic micro- and nano-structures have been investigated.<sup>39,51</sup> Using a micromanipulation technique, a helical SiGe nanostructure was demonstrated to have a linear dependence between applied force and extension. The reproducible extension of the helical structure supports the mechanical function of a spring-like structure, with a spring constant of 0.003 N/m and a resolution as low as 3 pN/nm. This property allows for application as a force sensor.

When a metallic helix deforms, not only spring constant but also electric properties (e.g., resistivity) varies. The change of electric properties can reflect the magnitude of external pressure. Arrays of Cr zigzag helical nanosprings on SiO<sub>2</sub>/Si were characterized as a pressure sensor.<sup>14</sup> When pressure is applied to the structure, the resistivity of the nanosprings drops because the physical touch of a neighboring nanospring provides a wider channel for electric current to flow. When the pressure is released, the nanosprings recover their initial resistivity. An overload pressure will cause irreversible plastic deformation of the nanosprings. As-synthesized nanosprings could be applied as pressure sensors to respond to a range of external forces. In another work, the piezoresistive behavior of SeGe nanohelices was observed, which also may be useful for force sensors because of their piezoelectricity.<sup>51</sup>

Pressure (or force) in other forms (e.g., fluidic flow) can also cause shape deformation of a nanospring. Li et al. designed superelastic metallic Ti microsprings as fluidic sensors and actuators.<sup>34</sup> The flow of a fluid could cause the length of the Ti microspring in a fluid channel to increase. The reversible length change of the Ti microspring was investigated using an alternating 0.3 and 0 m/s flow rate. The theoretical calculations of the microspring elongation as a function of the flow rate corroborate the experimental observations. The use of this mechanical property of the microspring could be feasible in future fluidic micro-/nano-device applications. In another work, the extension of a metal-coated Si micro-spring as a function of force was studied by Singh et al,<sup>39</sup> suggesting that the structure may be used as a sensor and an electromechanical actuator.

Palladium is an excellent material for sensing hydrogen. The sensing performance could be enhanced when the surface area of Pd material increases. Through AAO templating method, Yang et al. demonstrated that palladium helices exhibit better baseline stability, higher sensitivity, and lower power consumption in hydrogen sensing than solid palladium nanowires.<sup>20</sup>

### **Surface enhanced Raman spectroscopy (SERS)**

SERS is a surface-sensitive technique that enhances Raman scattering when molecules are adsorbed on a rough metal surface (e.g., silver and gold) and it is an ultrasensitive method to detect trace amounts of chemical and biological molecules. Two models of SERS mechanisms are commonly accepted, electromagnetic and chemical mechanisms. The largest enhancement was observed in narrow slits (hot spots) between two metals where a high local electric field exists. For a helical metallic structure, the distance between the wires of different turns or bends of zigzag helices may function as hot spots. From this point of view, flexible helical metal structures can be used to achieve a sensitive SERS signal by mechanical tuning. Zhou et al. investigated the SERS performance using helical silver zigzag-like nanorod arrays.<sup>17</sup> When the number of arms of the helical silver zigzag-like nanorods is less than 5, a sharp increase in the SERS intensity was observed. When greater than 5, the SERS intensity reached saturation. This phenomenon can be interpreted by the number change of effective hot spots. The top of the multiple arms can block the incident light to strike at the bottom hot spots in a silver nanorod film, which causes a disproportionate increase in the SERS intensity as the number of arms of the helical zigzag-like nanorods increases. The experimental results obtained from this work suggest that helical metal nano-structures could produce a large SERS intensity.

### **Surface plasmon resonance (SPR)**

SPR is a common phenomenon when microscopic noble metal particles meet electromagnetic light waves. SPR properties strongly correlate to the shape of microscopic noble metal particles. The microscopic noble metal particles with a helical shape are expected to generate unusual SPR properties. Ziegler et al. investigated the plasmonic response of gold nanoscale spirals.<sup>52</sup> The complex polarization response, resonance interactions and symmetry-breaking features were defined by the width and spacing of the spiral tracks, and by the winding number of the nanoscale Archimedean spirals.

### **Micro- and nano-machines**

A magnetic field is often used to manipulate the motion of magnetism-responsive metal helices by movement in a fluid.<sup>53</sup> Micro- and nano-scale robots with various shapes and components have been reviewed and are being expected applied in biomedical field thanks to their wireless manipulation ability via magnetic field.<sup>54-56</sup> Tottori and coworkers designed Ni/Ti bilayer-coated polymer helices.<sup>40</sup> The controlled motion of such a structure is propelled by an external magnetic field taking advantage of the magnetic shape anisotropy effect and magnetic actuation. The helix angle, magnitude of the magnetic field and frequency, and misalignment between the external magnetic field and helix determine the direction and velocity of the motion. An as-designed helical micromachine transported a colloidal microparticle to a target position as illustrated in Fig. 14. Wang et al. conducted a similar nanoswimmer study using Ni-coated Pd nanohelices.<sup>21</sup>

Kan and coworkers developed an electro-statically actuated helical Au-coated structure to tune the optical activity.<sup>36</sup> The planar micrometer-scale helices could be transformed to three-dimensional helices by adjusting the voltage between two ends of helices due to the deformation of helices under the electric field. This spatial change of the helices can be of use in tuning light in the terahertz frequency range.

### **Other applications**

Conventional metal coil structures can behave as an inductor when electric current passes through or an external magnetic field is applied. Therefore, the helical metallic micro- and nano-structures are likely usable as inductors. The electromagnetic induction properties of the Ag helix made from the vessel of a vascular plant were evaluated by measuring the direct-current (DC) conductivity and self-inductance. The evaluation results show that the as-synthesized helix structure could function as a solenoid with a DC conductivity of  $10^6$  S cm<sup>-1</sup> and a self-inductance approaching the level of picohenry.<sup>18</sup>



Experimental explorations helped finding many helical metallic micro- and nano-structures. Moreover, theoretical calculations on helical metallic micro- and nano-structures have predicted other applications and/or re-emphasized known applications of catalysis,<sup>57,58</sup> plasmonics,<sup>59-64</sup> mechanics,<sup>65</sup> electronics,<sup>66</sup> circular dichroism,<sup>67,68</sup> and reflection.<sup>69</sup>

#### **4 Summary**

Helical metallic micro- and nano-structures have been successfully demonstrated using GLAD, template-oriented, coating, rolled-up and self-assembly strategies; however, the fabrication of such structures remains challenging in terms of fine tuning the parameters of the structure and composition. These fabrication methods in all cited work on the theme are not general, just for specific metals. In the most of work conducted in the laboratory, advanced facilities and expensive materials are still necessary, which limits the further development of the field. Simpler methods independent of expensive apparatuses and materials may advance the practical fabrication and application of helical metallic micro- and nano-structures. Moreover, dimensions of metallic helices are unable to be controlled flexibly in the current stage. According to theoretical predictions and relevant experimental results reported in the literature, further investigations need to reveal the practicality of such structures in the use in such applications as chemical and biological sensors, actuators, photonic and electromagnetic devices, and micro- and nanomechanical systems. Considering the fabrication difficulty of helical metallic micro- and nano-structures, coating target metals on the helical structure is preferred as the fabrication is simple and well controlled. Helical metallic micro- and nano-structures exhibit an interesting morphology and unique properties. In particular, the micro- and nano-helices composed by metal atoms ensure the use beyond the utilization scope of organic helices.

#### **Acknowledgement**

This work was supported by the National Natural Science Foundation of China (NO. 21301072). S. Park thanks the support from the National Research Foundation of Korea (National Leading Research Lab: 2012R1A2A1A03670370).

**Reference:**

- 1 M. Subhramannia; V. K. Pillai, *J. Mater. Chem.*, 2008, **18**, 5858.
- 2 Y. Xiong; Y. Xia, *Adv. Mater.*, 2007, **19**, 3385.
- 3 T. S. Ahmadi; Z. L. Wang; T. C. Green; A. Henglein; M. A. El-Sayed, *Science*, 1996, **272**, 1924.
- 4 Y. Sun; Y. Xia, *Science*, 2002, **298**, 2176.
- 5 M. Grzelczak; J. Perez-Juste; P. Mulvaney; L. M. Liz-Marzan, *Chem. Soc. Rev.*, 2008, **37**, 1783.
- 6 E. Yashima; K. Maeda; H. Iida; Y. Furusho; K. Nagai, *Chem. Rev.*, 2009, **109**, 6102.
- 7 P. X. Gao; Y. Ding; W. Mai; W. L. Hughes; C. Lao; Z. L. Wang, *Science*, 2005, **309**, 1700.
- 8 B. A. Korgel, *Science*, 2005, **309**, 1683.
- 9 Y. Yang; Y. Zhang; Z. Wei, *Adv. Mater.*, 2013, **25**, 6039.
- 10 Y. Zhao; D. Ye; G.-C. Wang; T.-M. Lu: *Proc. of SPIE* **2003**, 5219, 59.
- 11 Y. He; Y. Zhao, *Nanoscale*, 2011, **3**, 2361.
- 12 K. Robbie; M. J. Brett; A. Lakhtakia, *Nature*, 1996, **384**, 616.
- 13 A. G. Mark; J. G. Gibbs; T.-C. Lee; P. Fischer, *Nat. Mater.*, 2013, **12**, 802.
- 14 S. V. Kesapragada; P. Victor; O. Nalamasu; D. Gall, *Nano Lett.*, 2006, **6**, 854.
- 15 Y. He; J. Fu; Y. Zhang; Y. Zhao; L. Zhang; A. Xia; J. Cai, *Small*, 2007, **3**, 153.
- 16 L. Chen; L. Andrea; Y. P. Timalina; G.-C. Wang; T.-M. Lu, *Cryst. Growth Des.*, 2013, **13**, 2075.
- 17 Q. Zhou; Y. He; J. Abell; Z. Zhang; Y. Zhao, *Chem. Comm.*, 2011, **47**, 4466.
- 18 K. Kamata; S. Suzuki; M. Ohtsuka; M. Nakagawa; T. Iyoda; A. Yamada, *Adv. Mater.*, 2011, **23**, 5509.
- 19 L. Liu; S.-H. Yoo; S. A. Lee; S. Park, *Nano Lett.*, 2011, **11**, 3979.
- 20 D. Yang; L. F. Fonseca, *Nano Lett.*, 2013, **13**, 5642.
- 21 J. Li; S. Sattayasamitsathit; R. Dong; W. Gao; R. Tam; X. Feng; S. Ai; J. Wang, *Nanoscale*, 2014, DOI: 10.1039/c3nr04760a.
- 22 Y. Wu; G. Cheng; K. Katsov; S. W. Sides; J. Wang; J. Tang; G. H. Fredrickson; M. Moskovits; G. D. Stucky, *Nat. Mater.*, 2004, **3**, 816.
- 23 J. K. Gansel; M. Thiel; M. S. Rill; M. Decker; K. Bade; V. Saile; G. von Freymann; S. Linden; M. Wegener, *Science*, 2009, **325**, 1513.
- 24 K. M. Manesh; S. Campuzano; W. Gao; M. J. Lobo-Castanon; I. Shitanda; K. Kiantaj; J. Wang, *Nanoscale*, 2013, **5**, 1310.
- 25 Y. Inoue; M. Uota; M. Uchigasaki; S. Nishi; T. Torikai; T. Watari; M. Yada, *Chem. Mater.*, 2008, **20**, 5652.
- 26 R. Takahashi; T. Ishiwatari, *Chem. Comm.*, 2004, 1406-1407.
- 27 D. J. Bell; Y. Sun; L. Zhang; L. X. Dong; B. J. Nelson; D. Grützmacher, *Sens. Actuators, A*, 2006, **130-131**, 54.
- 28 L. Zhang; L. Dong; D. J. Bell; B. J. Nelson; C. Schönenberger; D. Grützmacher, *Microelectron. Eng.*, 2006, **83**, 1237.
- 29 L. Dai; L. Zhang, *Nanoscale*, 2013, **5**, 971-976.
- 30 L. Zhang; D. Xu; L. Dong; B. J. Nelson, *Microelectron. Eng.*, 2009, **86**, 824.
- 31 D. J. Bell; T. E. Bauert; L. Zhang; L. X. Dong; Y. Sun; D. Grützmacher; B. J. Nelson, *Nanotechnology*, 2007, **18**, 055304.
- 32 L. Zhang; E. Ruh; D. Grützmacher; Dong; D. J. Bell; B. J. Nelson; C. Schönenberger, *Nano Lett.*, 2006, **6**, 1311.
- 33 L. Zhang; E. Deckhardt; A. Weber; C. Schönenberger; D. Grützmacher, *Nanotechnology*, 2005, **16**,

- 655.
- 34 W. Li; G. Huang; J. Wang; Y. Yu; X. Wu; X. Cui; Y. Mei, *Lab Chip*, 2012, **12**, 2322.
- 35 J. H. Singh; G. Nair; A. Ghosh, *Nanoscale*, 2013, **5**, 7224.
- 36 T. Kan; A. Isozaki; N. Kanda; N. Nemoto; K. Konishi; M. Kuwata-Gonokami; K. Matsumoto; I. Shimoyama, *Appl. Phys. Lett.*, 2013, **102**, 221906.
- 37 V. V. R. Sai; D. Gangadean; I. Niraula; J. M. F. Jabal; G. Corti; D. N. McIlroy; D. Eric Aston; J. R. Branen; P. J. Hrdlicka, *J. Phys. Chem. C*, 2010, **115**, 453.
- 38 G. D. Lilly; A. Agarwal; S. Srivastava; N. A. Kotov, *Small*, 2011, **7**, 2004.
- 39 J. P. Singh; D. L. Liu; D. X. Ye; R. C. Picu; T. M. Lu; G. C. Wang, *Appl. Phys. Lett.*, 2004, **84**, 3657.
- 40 S. Tottori; L. Zhang; F. Qiu; K. K. Krawczyk; A. Franco-Obregón; B. J. Nelson, *Adv. Mater.*, 2012, **24**, 811.
- 41 C. Zhan; J. Wang; J. Yuan; H. Gong; Y. Liu; M. Liu, *Langmuir*, 2003, **19**, 9440.
- 42 F. Qiu; L. Zhang; K. E. Peyer; M. Casarosa; A. Franco-Obregon; H. Choi; B. J. Nelson, *J. Mater. Chem. B*, 2014, **2**, 357.
- 43 G. Chang; G. Song; J. Yang; R. Huang; A. Kozinda; J. Shen, *Appl. Phys. Lett.*, 2012, **101**, 263505.
- 44 J. Fei; Y. Cui; A. Wang; P. Zhu; J. Li, *Chem. Comm.*, 2010, **46**, 2310.
- 45 Y. Yin; Y. Xia, *J. Am. Chem. Soc.*, 2003, **125**, 2048.
- 46 Y. Wang; Q. Wang; H. Sun; W. Zhang; G. Chen; Y. Wang; X. Shen; Y. Han; X. Lu; H. Chen, *J. Am. Chem. Soc.*, 2011, **133**, 20060.
- 47 C. Song; M. G. Blaber; G. Zhao; P. Zhang; H. C. Fry; G. C. Schatz; N. L. Rosi, *Nano Lett.*, 2013, **13**, 3256.
- 48 C.-L. Chen; N. L. Rosi, *J. Am. Chem. Soc.*, 2010, **132**, 6902.
- 49 C.-L. Chen; P. Zhang; N. L. Rosi, *J. Am. Chem. Soc.*, 2008, **130**, 13555.
- 50 J. Sharma; R. Chhabra; A. Cheng; J. Brownell; Y. Liu; H. Yan, *Science*, 2009, **323**, 112.
- 51 D. Grützmacher; L. Zhang; L. Dong; D. Bell; B. Nelson; A. Prinz; E. Ruh, *Microelectron. J.*, 2008, **39**, 478.
- 52 J. I. Ziegler; R. F. Haglund, *Nano Lett.*, 2010, **10**, 3013.
- 53 K. E. Peyer; S. Tottori; F. Qiu; L. Zhang; B. J. Nelson, *Chem. Eur. J.*, 2013, **19**, 28.
- 54 S. Sengupta; M. E. Ibele; A. Sen, *Angew. Chem. Int. Edit.*, 2012, **51**, 8434.
- 55 S. Sánchez; M. Pumera, *Chem. Asian J.*, 2009, **4**, 1402.
- 56 K. E. Peyer; L. Zhang; B. J. Nelson, *Nanoscale*, 2013, **5**, 1259.
- 57 W. An; Y. Pei; X. C. Zeng, *Nano Lett.*, 2007, **8**, 195.
- 58 J. Yang; B. Li; Q. Zhang; W.-I. Yim; L. Chen, *J. Phys. Chem. C*, 2012, **116**, 11189.
- 59 Z. Fan; A. O. Govorov, *Nano Lett.*, 2012, **12**, 3283.
- 60 J. Ziegler; R. Haglund, Jr., *Plasmonics*, 2013, **8**, 571.
- 61 Y. R. Li; R. M. Ho; Y. C. Hung, *IEEE Photonics J.*, 2013, **5**, 2700510.
- 62 Z. Y. Zhang; Y. P. Zhao, *J. App. Phys.*, 2008, **104**, 013517.
- 63 Z. Y. Zhang; Y. P. Zhao, *Appl. Phys. Lett.*, 2007, **90**, 221501.
- 64 J. Trevino; H. Cao; L. Dal Negro, *Nano Lett.*, 2011, **11**, 2008.
- 65 A. F. da Fonseca; D. S. Galvao, *Phys. Rev. Lett.*, 2004, **92**, 175502.
- 66 T. Kosugi, *J. Phys. Soc. Jpn.*, 2013, **82**, 034703.
- 67 S. Droulias; V. Yannopapas, *J. Phys. Chem. C*, 2013, **117**, 1130.
- 68 D. Moore; J. I. Tinoco, *J. Chem. Physics*, 1980, **72**, 3396.

69 Z. Lu; M. Zhao; P. Xie; L. Wu; Y. Yu; P. Zhang; Z. Yang, *J. Lightwave Technol.*, 2012, **30**, 3050.

## Figures

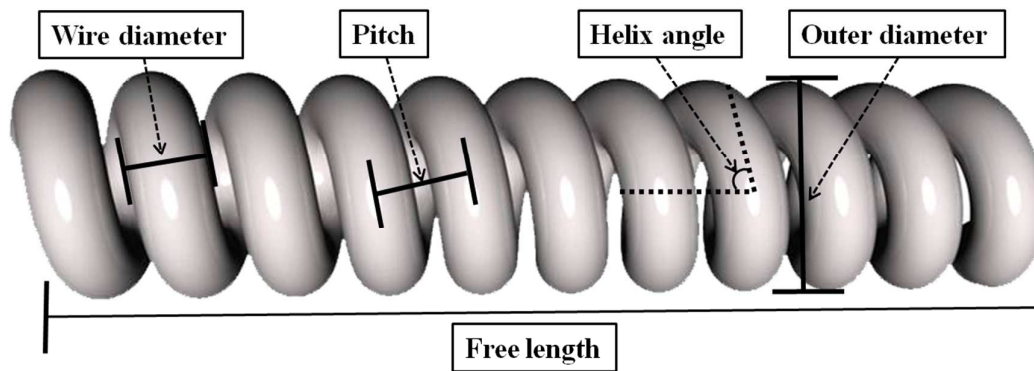


**Fig. 1** Schematic presentation of a typical helical coil structure with elliptic cross-section.

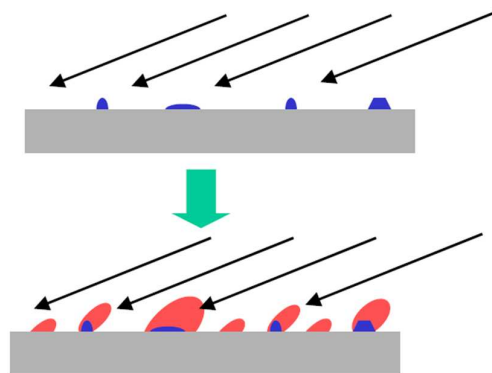


**Figure 2** The shadowing effect during oblique angle deposition: (a) initial nucleation to form shadowing centers; and (b) columnar structures formed due to the shadowing effect. (Reproduced with permission from ref 10.)

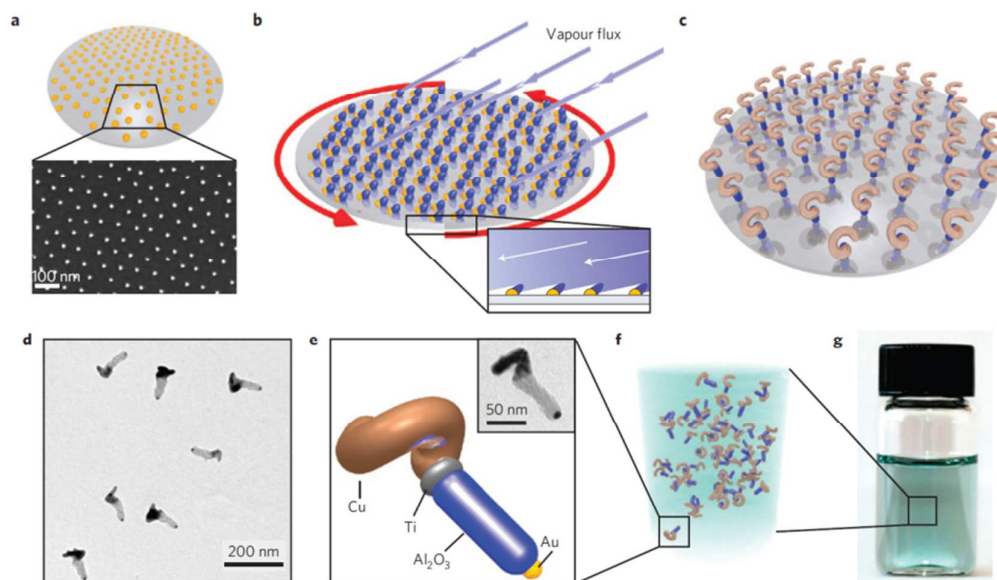


**Figure 3** Fabrication scheme illustrated for nanohooks with  $C_1$  symmetry. **a,b**, The 14 nm gold nanodots patterned by micellar nanolithography (**a**, bottom, SEM image of patterned wafer) act as nucleation sites (**b**) during subsequent shadow growth. **c**, Manipulation of the substrate angle and deposition material creates complex 3D structures. The growth process takes approximately 1 h. **d**, TEM image of hybrid insulator–metal nanohooks. **e**, Model of the designed structure, and TEM image showing the grown structure (inset). **f,g**, On sonication the nanoparticles are released into solution (schematic (**f**), photograph (**g**)). (Adapted with permission from ref 13)



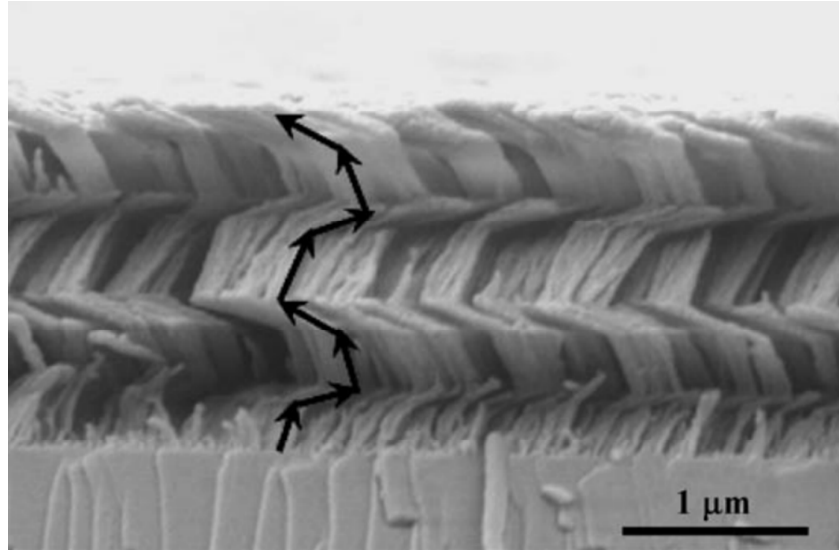


**Figure 4** SEM images of the multilayered Si/Ni nanosprings grown on a Si(100) substrate.

(Adapted with permission from ref 15)

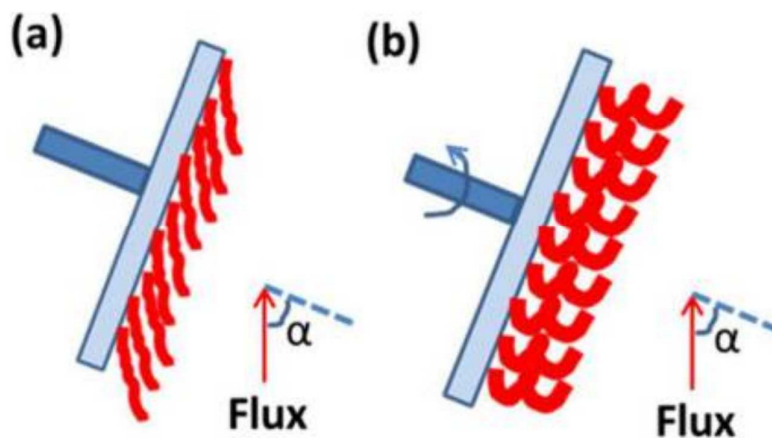


**Figure 5** (a) Schematic showing a stationary OAD configuration with no substrate rotation and a fixed incident flux angle  $\alpha$ . Typically a slanted rod-like structure inclined toward the incident flux is formed. (b) Dynamic OAD configuration where the substrate is rotated around the surface normal during deposition while the incident flux angle  $\alpha$  is fixed. A spiral structure can be grown. (Adapted with permission from ref 16)

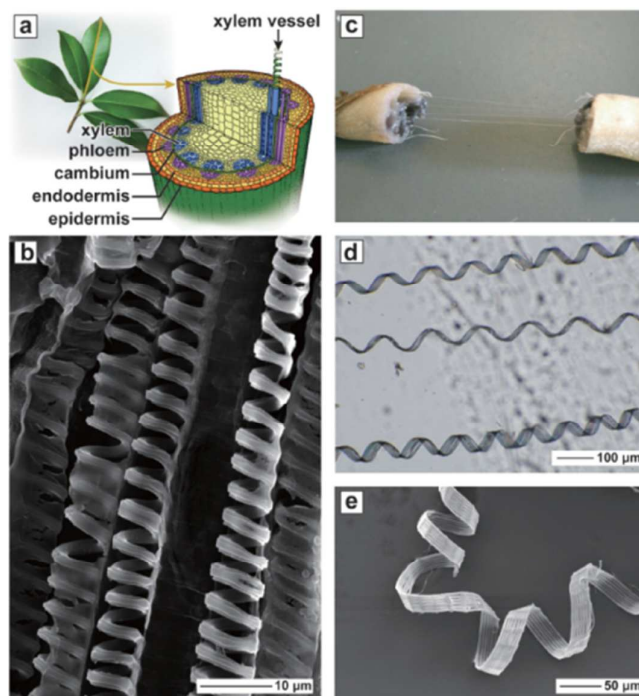


**Figure 6** (a) Schematic illustration of cross-section of plant tissue in dicotyledoneae. The spiral vessels exist in part of xylem to support water transportation as secondary wall of vessel. (b) SEM image of spiral vessels housed in leaf tissue of *Photinia fraseri* (red robin). The sample was prepared by cutting a part of leaf vein into strips without any other treatment for isolation of the spiral vessels. Helical microstructure was found with the dimensions of 4–10  $\mu\text{m}$  in  $D$  and 5–10  $\mu\text{m}$  in  $l/N$ . (c) Photograph of white fibers drawn from cross sections of rhizome of *Nelumbo nucifera* (lotus). The  $l$  of white fiber can be controlled by distance between the two pieces of rhizomes. (d) Optical microscopy image of the white fiber, indicating individual spiral vessels without entanglement. (e) SEM image of one spiral vessel, showing multiple helical structure uniting single springs with diameter of 5  $\mu\text{m}$ , just similar to coiled-ribbon structure. Seven single springs form bundle arrangement, thus the width of spiral vessel was around 35  $\mu\text{m}$ . The other structural parameters were  $D=50\text{--}80$   $\mu\text{m}$  and  $l/N=50\text{--}100$   $\mu\text{m}$ . (Adapted with permission from ref 18)

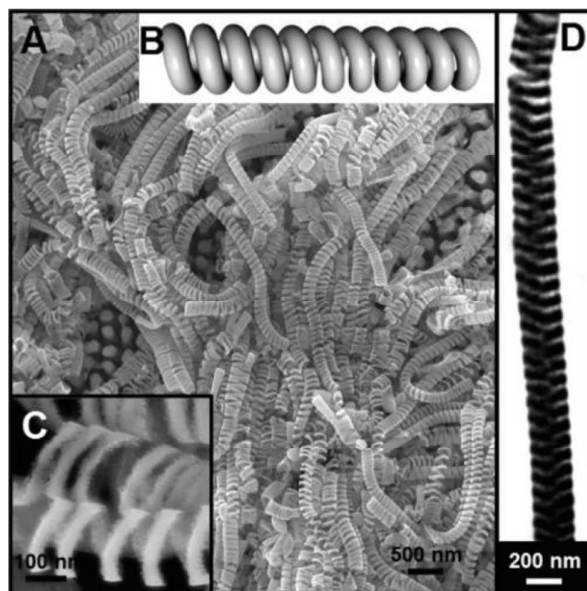


**Figure 7** (A) SEM image of large quantity of Pd nanosprings synthesized using  $\sim 250$  nm nanochannel of commercial AAO template. (B) A drawing of real spring structure. (C) Magnified SEM image of Pd nanosprings showing their clear spring shapes. (D) TEM image of a typical Pd nanospring with  $\sim 60$  nm in wire diameter and  $\sim 238$  nm in spring diameter. (Adapted with permission from ref 19)

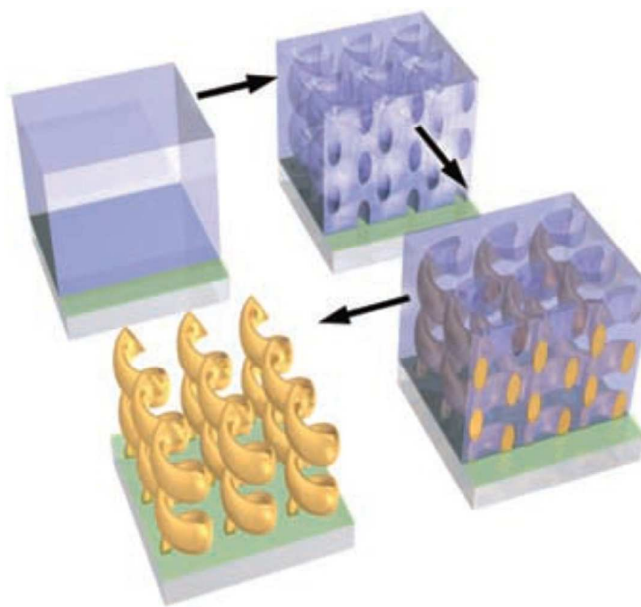


**Figure 8** A positive-tone photoresist (blue) is spun onto a glass substrate covered with a 25-nm thin film of conductive indium-tin oxide (ITO) shown in green. After 3D DLW and development, an array of air helices in a block of polymer results. After plating with gold in an electrolyte, the polymer is removed by plasma etching, leading to a square array of freestanding 3D gold helices. (Adapted with permission from ref 23)

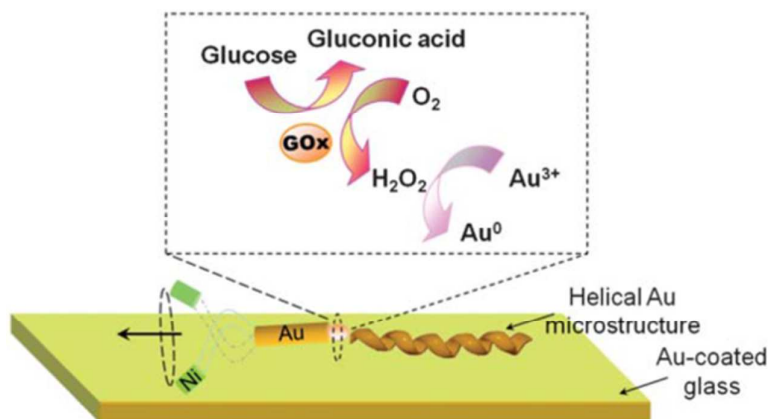


**Figure 9** Schematic representation of the nanomotor-induced biocatalytic metallization of a helical Au microstructure using a GOx-Au/Ag<sub>flex</sub>/Ni magnetic nanowire swimmer. Inset shows the biocatalytic reactions involved in the Au patterning. (Adapted with permission from ref 24)

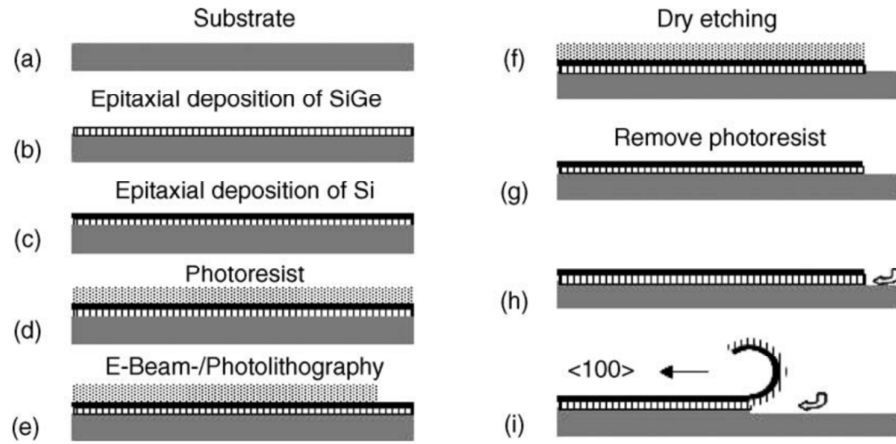


**Figure 10** Basic process sequence: initial planar bilayer, patterned through conventional microfabrication techniques assembles itself into 3D nanostructures during wet etch release.

(Adapted with permission from ref 27)

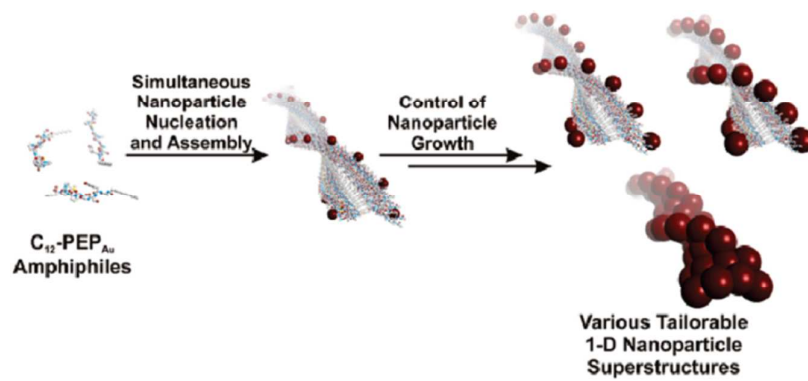


**Figure 11** Nanoparticle Synthesis and Assembly Strategy. (Adapted with permission from ref 48)



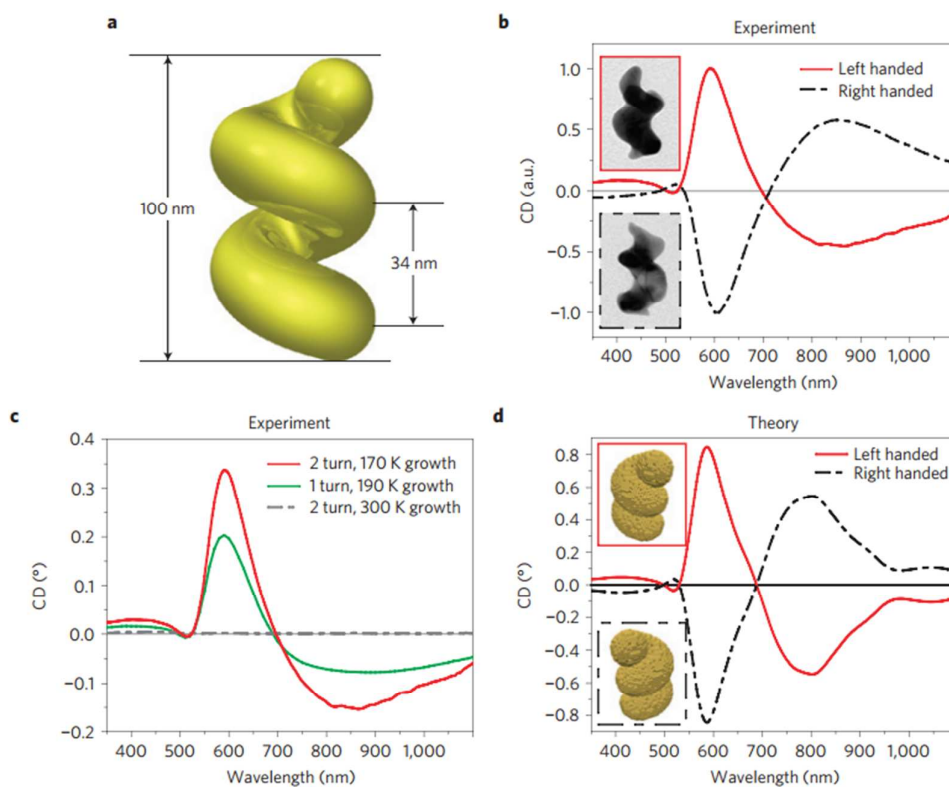


**Figure 12** The chiroptical response of solutions of Au nanohelices. a, Model two-turn gold nanohelix showing critical dimensions. b, Normalized circular dichroism (CD) spectra of left-handed and right-handed helices. Inset: TEM images of grown structures with left (top) and right (bottom) chirality (image dimensions: 85 nm×120 nm). c, Circular dichroism spectra of two- and one-turn helices grown under cooling conditions, and of nominal two-turn helices grown at room temperature. The spectra are plotted against an absolute y axis calibrated according to the optical density of the max peaks (at around 600 nm) in the corresponding ultraviolet–visible spectra. d, Simulated CD spectra for a based on model dimensions taken from TEM images. The insets show the discrete dipole models used in the calculations. (adapted with permission from ref 13)

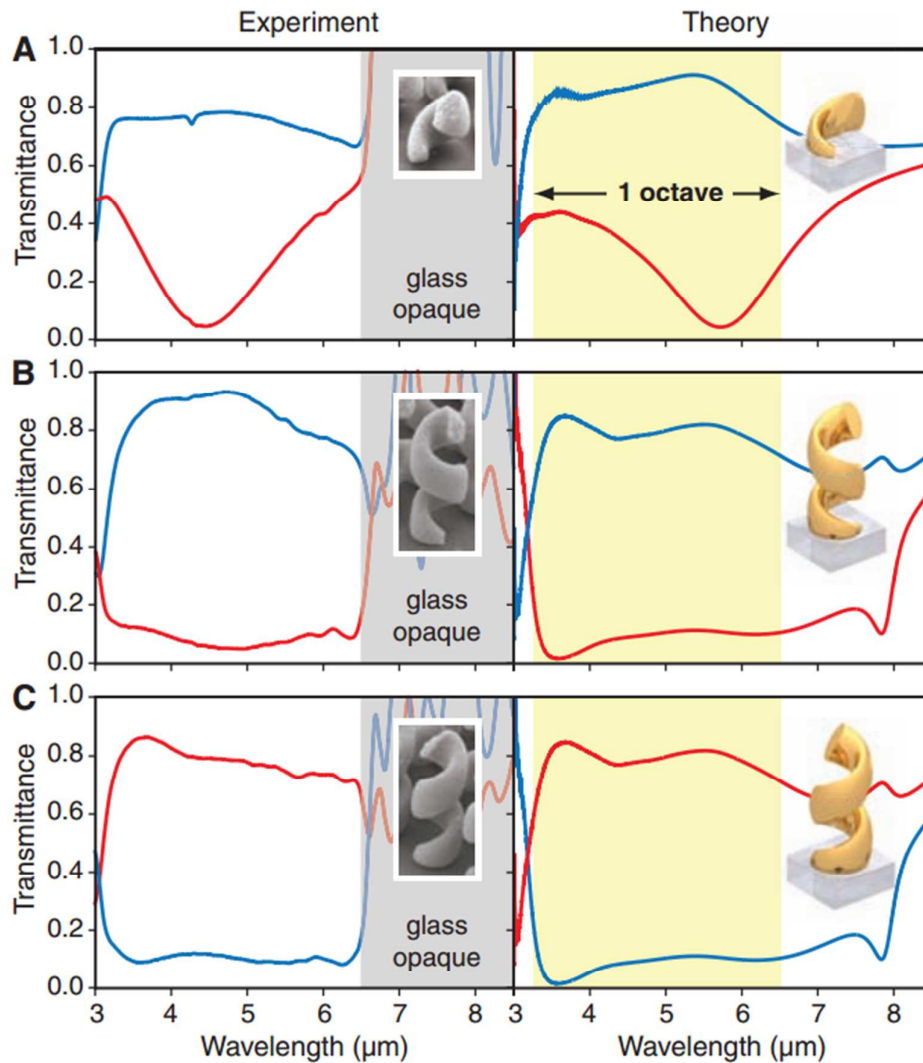


**Figure 13** Normal-incidence measured and calculated transmittance spectra (no analyzer behind sample) are shown in the left and right columns. LCP and RCP are depicted in red and blue, respectively. (A) Slightly less than one pitch of left-handed helices, (B) two pitches of left-handed helices, and (C) Two pitches of right-handed helices (see insets). For wavelengths longer than  $6.5 \mu\text{m}$ , the glass substrate in the experiments becomes totally opaque. Hence, transmittance cannot be measured. For wavelengths below  $3 \mu\text{m}$ , light can be diffracted into the glass substrate ( $a=2 \mu\text{m}$  and refractive index  $n=1.5$ ), giving rise to Wood anomalies. (adapted with permission from ref 23)

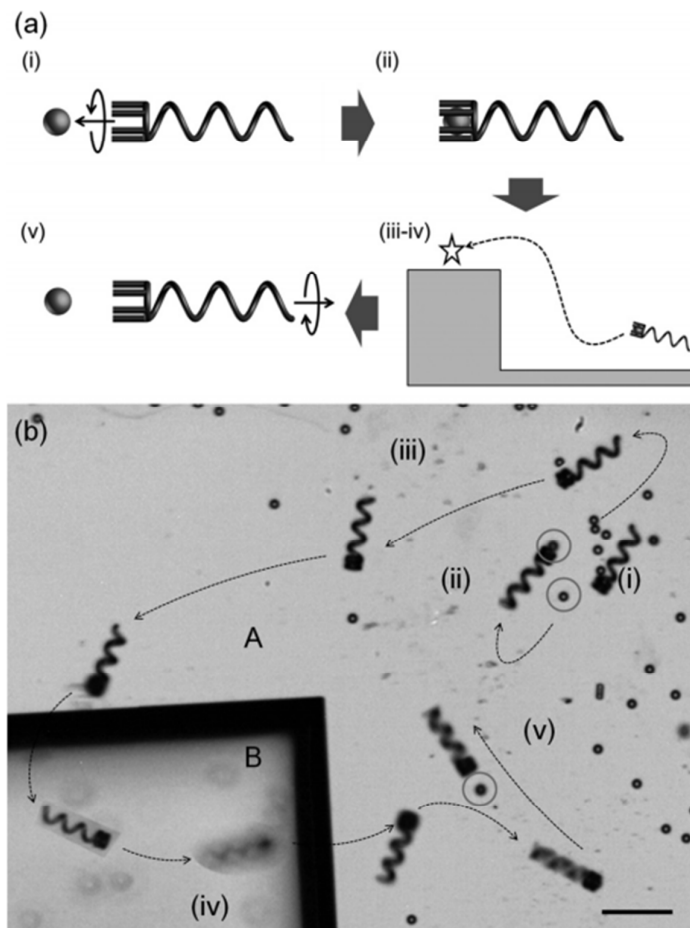


**Figure 14** a) Illustration of transportation procedure by a helical micromachine with a microholder. b) Time-lapse image of the pick-and-place micromanipulation of a 6  $\mu\text{m}$  diameter microparticle. The circles indicate the selected microparticle. The scale bar is 50  $\mu\text{m}$ . (adapted with permission from ref 52)